

Group theoretical treatment of the low-temperature phase transition of the Cd_6Ca 1/1-cubic approximant

R. Tamura,¹ K. Edagawa,² K. Shibata,¹ K. Nishimoto,¹ S. Takeuchi,¹ K. Saitoh,³ M. Isobe,⁴ and Y. Ueda⁴

¹*Department of Materials Science and Technology, Tokyo University of Science, Noda, Chiba 278-8510, Japan*

²*Institute of Industrial Science, The University of Tokyo, Komaba, Meguro-ku, Tokyo 153-8505, Japan*

³*Ecotopia Science Institute, Nagoya University, Nagoya 464-8603, Japan*

⁴*Institute for Solid State Physics (ISSP), The University of Tokyo, Kashiwa, Chiba 277-8581, Japan*

(Received 7 October 2005; published 29 November 2005)

An antiparallel orientational transition is reported for an intermetallic compound, i.e., Cd_6Ca crystal, which is a 1/1–1/1–1/1 crystalline approximant to the icosahedral quasicrystal $\text{Cd}_{5,7}\text{Ca}$. A group theoretical analysis based on the Landau theory predicts that the space group of the low-temperature phase is either $C2/c$ or $C2/m$, in good agreement with the observations. Accordingly, two types of orientational orderings of Cd_4 tetrahedra, which are located in the center of icosahedral clusters, may occur below 100 K: In both cases, the Cd_4 tetrahedra are orientationally ordered in an antiparallel fashion along the [110] direction of the high temperature body-centered-cubic phase. Such a transition in a metal is reminiscent of orientational transitions in *molecular solids*.

DOI: [10.1103/PhysRevB.72.174211](https://doi.org/10.1103/PhysRevB.72.174211)

PACS number(s): 61.44.Br, 61.10.Nz, 61.14.–x, 64.60.–i

I. INTRODUCTION

Recently, an occurrence of a structural phase transition has been reported^{1,2} at a very low temperature for the Cd_6Ca and Cd_6Yb crystals,³ which are crystalline analogs, i.e., 1/1 cubic approximants, to the *binary* icosahedral $\text{Cd}_{5,7}\text{Ca}$ and $\text{Cd}_{5,7}\text{Yb}$.^{4,5} The obtained transition entropies for these two compounds⁶ have suggested that the transitions are an order-disorder type over two configurations per icosahedral cluster, which builds up a bcc lattice with additional “glue” atoms.^{7,8} For the origin of the phase transitions, substantial attention has been paid to an orientationally disordered Cd_4 tetrahedron located in the center of the icosahedral clusters. Recent x-ray refinements on a series of Cd_6M ($M=\text{Ca}$, rare earth) compounds by Gomez and Lidin⁹ have clearly confirmed the existence of such disorder at room temperature and have also revealed variations in the disorder, which was modeled by combinations of two types of disorders, i.e., type 1 and type 2: The type-1 disorder is a 90° rotational disorder along a twofold axis of the tetrahedron and the type-2 is described as a triple split of the tetrahedral corner atoms. Both type-1 and type-2 disorders coexist at room temperature for Cd_6Ca and Cd_6Yb and because of this inherent disorder, the phase transitions are expected to be a consequence of orientational ordering of the Cd_4 tetrahedra. This should be a novel type of phase transition in an intermetallic compound, reminiscent of orientational transitions in molecular solids. However, their transition mechanism as well as the superstructure formed at low temperatures has been an intriguing puzzle up to date, partly because the structural change accompanying the transition is extremely small. In this paper, we will first present results of low temperature x-ray and electron diffraction experiments on a single grained Cd_6Ca , then describe the phase transition group theoretically based on the Landau theory, and finally present a possible superstructure which is consistent with the experiments.

II. EXPERIMENT

Pure elements of Cd (6N) and Ca (4N) near the composition Cd_6Ca were melted at 973 K for 24 h in an alumina crucible sealed inside a quartz tube under an argon atmosphere. The ingots were then slowly cooled from the melt at the rate of -1 K/h to grow single grains from the Cd melt. The obtained single grains exhibit clearly defined facets, surrounded by {100} and {110} surfaces. X-ray diffraction measurements were performed using Cu $K\alpha$ radiation at temperatures between 10 and 300 K in the 2θ - θ scanning mode with the incident angle θ to a {100} and {611} surfaces. TEM observations were performed using JEM2010F equipped with a liquid N_2 cooling stage operating at an acceleration voltage of 200 kV.

III. X-RAY DIFFRACTION

Figure 1 presents x-ray diffraction spectra around the 18 0 0 peak of a single-grained Cd_6Ca at temperatures between 10 and 180 K. It is seen that with decreasing temperatures the single peak is split into two peaks at 100 K, which clearly shows that the low temperature phase is neither cubic nor trigonal. Figure 2 presents x-ray diffraction spectra around 18 3 3 peak of a single-grained Cd_6Ca at 300 and 10 K. For the spectrum at 10 K, the split peaks are successfully decomposed into four components using Lorentzian functions, which manifests that the {18 3 3} planes with 24 multiplicities under the space group $Im\bar{3}$ are decomposed into four nonequivalent planes, or more, below 100 K. Here we note that in the cases of the orthorhombic, the monoclinic, and the triclinic lattices, which are the subgroups of the high temperature phase ($Im\bar{3}$), the multiplicity of the {18 3 3} planes for each Laue group is 8, 4, and 2, respectively. Therefore, the 18 3 3 peak would in principle be split into 3, 6, and 12 peaks upon phase transition, respectively. For this reason splitting into more than three peaks indicates that the low-

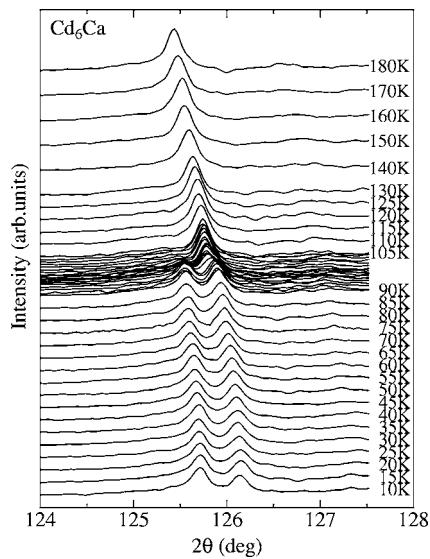


FIG. 1. Cu $K\alpha$ x-ray diffraction profiles of the 18 0 0 peak with the incident angle θ to the (100) surface of a single-grained Cd_6Ca in the 2θ - θ scanning mode. The spectra were taken from 10 to 180 K with increasing temperature. For the profiles between 90 and 105 K, the temperature step is 1 K.

temperature phase possesses a monoclinic or a triclinic lattice. Here we note that such a conclusion obtained by using a single grain may not be reached by standard powder x-ray diffraction experiments since a number of nonequivalent reflections contribute to a single peak for the latter case. For instance, five nonequivalent reflections contribute to a peak at the same angle as the 18 0 0 reflection, and nine nonequivalent reflections are superimposed on the 18 3 3 reflection. These nonequivalent reflections would split in a different manner at the transition, making it difficult to obtain direct information on the low-temperature phase.

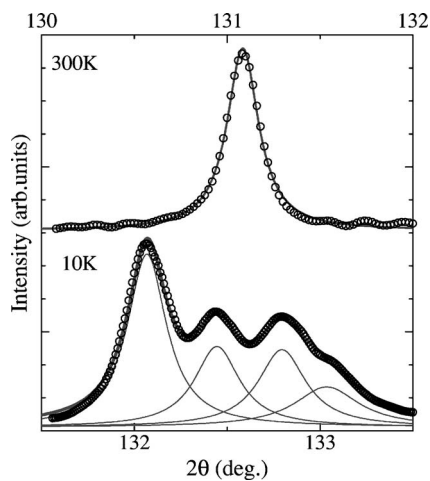


FIG. 2. X-ray diffraction spectra of the 18 3 3 peak of a single-grained Cd_6Ca at 300 and 10 K. Decomposition of the spectrum at 10 K is performed by a least square fit (solid lines) using Lorentzian functions.

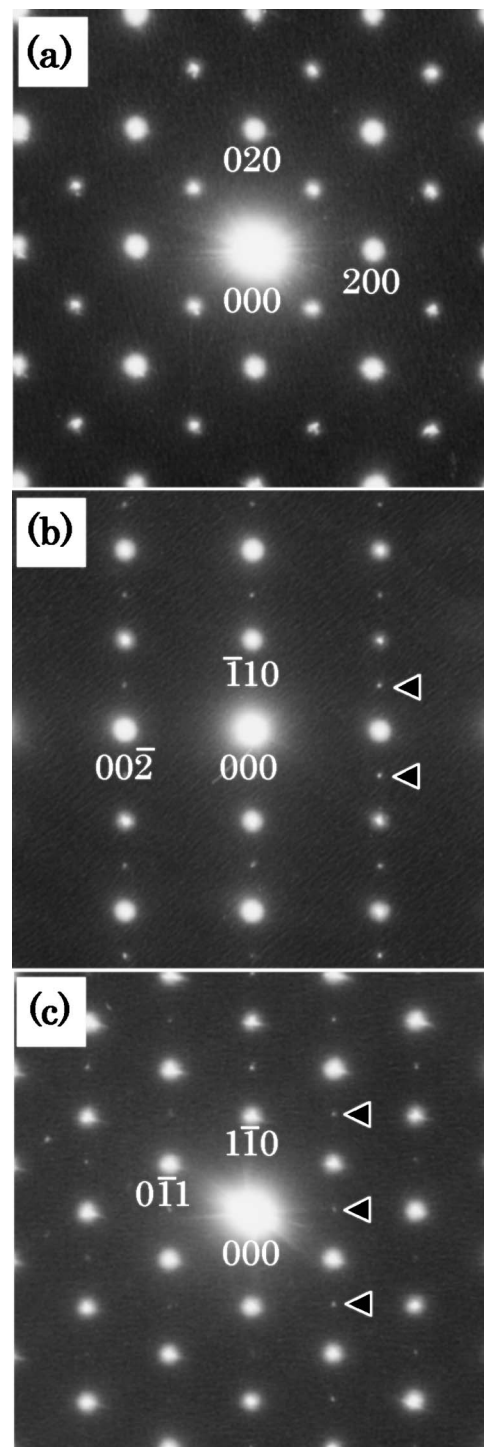


FIG. 3. Electron diffraction patterns of Cd_6Ca taken along (a) [001], (b) [110], and (c) [111] directions at 80 K. In (b) and (c), superlattice reflections are seen at midpoints of the fundamental spots, as marked by solid triangles.

IV. ELECTRON DIFFRACTION

Figures 3(a)–3(c) present electron diffraction patterns of Cd_6Ca taken along [001], [110], and [111] directions at about 80 K. We observe that superlattice reflections appear at positions $h+1/2, k+1/2, l$ in the [110] and [111] incidences, which means that the periodicity in the [110] direction is

TABLE I. Character table of the small representations for the N point.

	E	C_2	i	σ_h
N_1^+	1	1	1	1
N_2^+	1	-1	1	-1
N_1^-	1	1	-1	-1
N_2^-	1	-1	-1	1

doubled below the transition temperature. Figure 3(c) clearly demonstrates that the threefold symmetry is broken by an appearance of superlattice spots below 100 K, which is consistent with the cubic-symmetry breaking observed by the x-ray diffraction experiment. In addition, as seen in Fig. 3(b), spots with l =odd are absent in the low-temperature phase. Taking into consideration that there is one Bravais lattice, i.e., a primitive one, for the triclinic system and there are two Bravais lattices, i.e., a primitive and a C -centered one, for the monoclinic system, the observed extinction in Fig. 3(b) can only be explained by a C -centered monoclinic lattice with the b axis, the unique axis, parallel to the c axis of the high-temperature phase (2nd setting). In Fig. 3(b), $h\bar{h}l$ of the bcc lattice are indexed as $2\bar{h}l0$ of the C -centered lattice with a double unit cell ($\sqrt{2}a \times a \times \sqrt{2}a$). Because of the reflection condition hkl : $h+k$ =even due to the C centering, $2\bar{h}l0$ reflections disappear when l =odd, which explains the pattern in the $[110]$ incidence. The absence of $hk0$ spots with $h+k$ =odd in the $[001]$ incidence can also be explained in this manner: $hk0$ of the high-temperature phase are indexed as $\bar{h}+k0h+k$ of the C -centered lattice with a double unit cell and these spots disappear when $h+k$ =odd due to the C centering. Thus, from the diffraction experiments we are led to a conclusion that the low-temperature phase is a C -centered monoclinic phase with a double unit cell.

V. PHENOMENOLOGICAL ARGUMENTS BASED ON THE LANDAU THEORY

Next, we discuss the symmetry of the low-temperature phase by a group theoretical method based on the Landau theory.¹⁰ The appearance of $h+1/2$, $k+1/2$, l superlattice reflections in Cd_6Ca is attributed to a basis, or its linear combination, of an irreducible representation (irrep) of the high-symmetry group $G_0(\equiv \text{Im}\bar{3})$ at $N(\pi/a \pi/a 0)$. The star of \vec{k} at N contains the following six vectors; $\vec{k}_1=(\pi/a \pi/a 0)$, $\vec{k}_2=(\pi/a -\pi/a 0)$, $\vec{k}_3=(0 \pi/a \pi/a)$, $\vec{k}_4=(0 \pi/a -\pi/a)$, $\vec{k}_5=(\pi/a 0 \pi/a)$, $\vec{k}_6=(-\pi/a 0 \pi/a)$. The group of \vec{k}_i (leaving \vec{k}_i invariant) is $2/m$ and there are four one-dimensional small representations for $2/m$ as listed in Table I; N_1^+ , N_2^+ , N_1^- , N_2^- . Each irrep N of the space group G_0 is six dimensional with six basis functions ϕ_i ($i=1, \dots, 6$). Since continuous transitions are not allowed for the N_1^+ and N_2^+ irreps because of the existence of a third-order invariant (the Landau condition), the present phase transition is attributed to either N_1^- or N_2^- irrep within the framework of the

Landau theory. The order parameter which belongs to the N_1^- irrep transforms under the generators of the group $\text{Im}\bar{3}$ as follows:

$$\begin{aligned}
 & i: \phi_i \rightarrow -\phi_i \quad (i=1, \dots, 6) \\
 & C_2([100]): \phi_1 \rightarrow \phi_2, \phi_2 \rightarrow \phi_1, \phi_3 \rightarrow \phi_3, \phi_4 \rightarrow \phi_4, \\
 & \quad \phi_5 \rightarrow \phi_6, \phi_6 \rightarrow \phi_5, \\
 & C_3([111]): \phi_1 \rightarrow \phi_5, \phi_2 \rightarrow \phi_6, \phi_3 \rightarrow \phi_1, \phi_4 \rightarrow \phi_2, \\
 & \quad \phi_5 \rightarrow \phi_3, \phi_6 \rightarrow \phi_4, \\
 & t\left(\left[\frac{1}{2} \frac{1}{2} \frac{1}{2}\right]\right): \phi_1 \rightarrow -\phi_1, \phi_2 \rightarrow \phi_2, \phi_3 \rightarrow -\phi_3, \phi_4 \rightarrow \phi_4, \\
 & \quad \phi_5 \rightarrow -\phi_5, \phi_6 \rightarrow \phi_6, \tag{1}
 \end{aligned}$$

and the order parameter which belongs to the N_2^- irrep transforms as follows:

$$\begin{aligned}
 & i: \phi_i \rightarrow -\phi_i \quad (i=1, \dots, 6), \\
 & C_2([100]): \phi_1 \rightarrow -\phi_2, \phi_2 \rightarrow -\phi_1, \phi_3 \rightarrow -\phi_3, \\
 & \quad \phi_4 \rightarrow -\phi_4, \phi_5 \rightarrow \phi_6, \phi_6 \rightarrow \phi_5, \\
 & C_3([111]): \phi_1 \rightarrow \phi_5, \phi_2 \rightarrow \phi_6, \phi_3 \rightarrow \phi_1, \phi_4 \rightarrow \phi_2, \\
 & \quad \phi_5 \rightarrow \phi_3, \phi_6 \rightarrow \phi_4, \\
 & t\left(\left[\frac{1}{2} \frac{1}{2} \frac{1}{2}\right]\right): \phi_1 \rightarrow -\phi_1, \phi_2 \rightarrow \phi_2, \phi_3 \rightarrow -\phi_3, \phi_4 \rightarrow \phi_4, \\
 & \quad \phi_5 \rightarrow -\phi_5, \phi_6 \rightarrow \phi_6, \tag{2}
 \end{aligned}$$

where $C_l([\dots])$ is an l -fold rotation along the direction $[\dots]$, i is the inversion, and $t\left(\left[\frac{1}{2} \frac{1}{2} \frac{1}{2}\right]\right)$ is a translation of $(\frac{1}{2}, \frac{1}{2}, \frac{1}{2})a$. Both order parameters have four fourth-order invariants and the Landau free energy is given by the following expression to the fourth order for both irreps,

$$\begin{aligned}
 \Phi = & \Phi_0 + A\eta^2 + B_1\eta^4 + B_2\eta^4(\gamma_1^4 + \gamma_2^4 + \gamma_3^4 + \gamma_4^4 + \gamma_5^4 + \gamma_6^4) \\
 & + B_3\eta^4(\gamma_1^2\gamma_2^2 + \gamma_3^2\gamma_4^2 + \gamma_5^2\gamma_6^2) + B_4\eta^4(\gamma_1\gamma_2\gamma_3\gamma_4 \\
 & + \gamma_3\gamma_4\gamma_5\gamma_6 + \gamma_5\gamma_6\gamma_1\gamma_2), \tag{3}
 \end{aligned}$$

where Φ_0 is the free energy of the high-symmetry phase, η the magnitude of the order parameter, and $\sum_{i=1}^6 \gamma_i^2 = 1$. Then the low-symmetry phase is described by $\psi = \sum_{i=1}^6 \gamma_i \phi_i$.

Minimization of Φ with respect to the γ_i ($i=1, \dots, 6$) variables yields a variety of cases depending on the values of B_2 , B_3 , and B_4 . However, as seen in Fig. 3(c), the superlattice reflections appear only at $h+1/2$, $k+1/2$, l , but not at h , $k+1/2$, $l+1/2$ and $h+1/2$, k , $l+1/2$ positions simultaneously, which means that we can set $\gamma_3 = \dots = \gamma_6 = 0$. Therefore, among all the cases that minimize Eq. (3), the present transition is attributed to either of the following two cases:

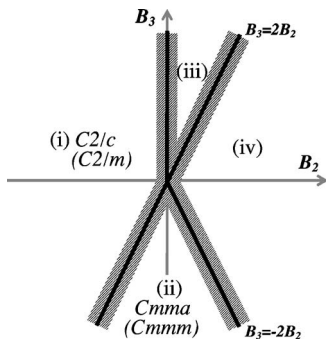


FIG. 4. A section of the phase diagram of the low-symmetry phases at $B_4=0$, resulting from the N_1^- (N_2^-) irrep of the space group $Im\bar{3}$. Space groups in parentheses represent those obtained from the N_2^- irrep. B_2 , B_3 , and B_4 are the coefficients of the fourth-order invariants in the Landau free energy expansion [Eq. (3)]. Cases (iii) and (iv) correspond to γ_1^2 (or γ_2^2) = γ_3^2 (or γ_4^2) = γ_5^2 (or γ_6^2) = $1/3$ and $\gamma_1^2 = \dots = \gamma_6^2 = 1/6$, respectively.

$$(i) B_2 < 0, B_3 > 2B_2, 10B_2 - B_3 < B_4 < -12B_2 + 2B_3:$$

$$\gamma_1^2 = 1, \gamma_2 = \dots = \gamma_6 = 0 \quad \text{or} \quad \gamma_2^2 = 1, \gamma_1 = \gamma_3 = \dots = \gamma_6 = 0;$$

$$(ii) B_2 < 0, B_3 < 2B_2, 4B_2 + 2B_3 < B_4 < -4B_2 - 2B_3$$

$$\text{or } B_2 > 0, B_3 < -2B_2, 4B_2 + 2B_3 < B_4 < -4B_2 - 2B_3:$$

$$\gamma_1^2 = \gamma_2^2 = \frac{1}{2}, \gamma_3 = \dots = \gamma_6 = 0. \quad (4)$$

A section of the resulting phase diagram at $B_4=0$ is illustrated in Fig. 4. For the case (i), the low-symmetry phase is given by $\psi = \phi_1$ or ϕ_2 , which results in a C -centered monoclinic lattice with space groups $C2/c$ and $C2/m$ from the N_1^- and the N_2^- irreps, respectively. For the case (ii), the low-symmetry phase is given by $\psi = (1/\sqrt{2})(\phi_1 \pm \phi_2)$, which leads to a C -centered orthorhombic lattice with space groups $Cmma$ and $Cmmm$ from the N_1^- and the N_2^- irreps, respectively. Of these two cases, the occurrence of a C -centered monoclinic lattice at low temperatures is explained by case (i).

The next interesting question is what type of ordering is compatible with the symmetries obtained from the Landau theory. Since any order parameter which belongs to \bar{k}_i should transform as a basis of an irrep of $2/m$, only two cases are allowed to occur with respect to the orientation of the Cd_4 tetrahedron: Either a twofold axis of the tetrahedron is parallel to the b axis of the monoclinic lattice or a mirror of the tetrahedron is perpendicular to the b axis. Accordingly, two types of superstructures are possible from case (i), which are schematically illustrated in Figs. 5(a) and 5(b), respectively. In the case of $C2/c$, a twofold rotational symmetry is preserved at the transition and thus a twofold axis of the Cd_4 tetrahedra is parallel to the b axis of the monoclinic lattice as shown in Fig. 5(a), whereas in the case of $C2/m$ a mirror symmetry is preserved and mirrors of the Cd_4 tetrahedra are perpendicular to the b axis as shown in Fig. 5(b). In both

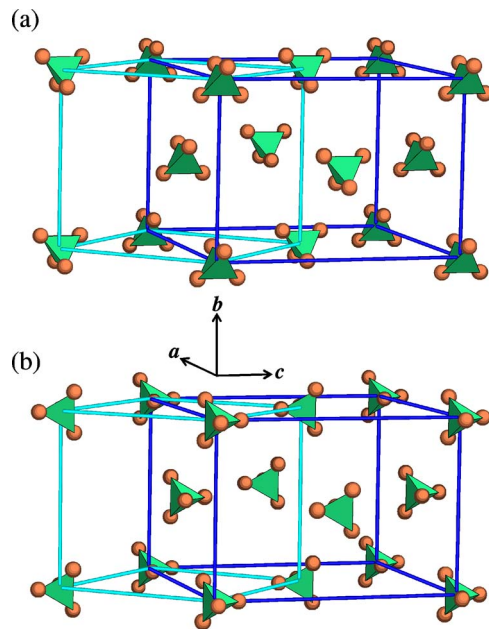


FIG. 5. (Color online) Schematic illustrations of two types of superstructures below 100 K with respect to the orientation of the Cd_4 tetrahedra, obtained from case (i): (a) $C2/c$ and (b) $C2/m$ -type ordering, respectively. Only the Cd_4 tetrahedra are shown in the figures and the faces of the tetrahedra are colored for clarity. In both figures, the unit cell of the C -centered monoclinic phase (2nd setting) is marked by black lines and light gray lines indicate the unit cell of the high-temperature bcc phase. In (b) a mirror of the Cd_4 tetrahedra is perpendicular to the b axis of the monoclinic lattice, and arbitrary rotation of the tetrahedra along the b axis is allowed.

cases, ordering of the Cd_4 tetrahedra takes place over two orientations along the $[1\ 1\ 0]$ direction of the high-temperature phase. Here, we note that the space groups $C2/m$ and $C2/c$ differ by the reflection condition $h0l: l = 2n$. With this respect, electron diffraction patterns taken along $[010]$ direction at 80 K do not reveal any superlattice spots, which supports an occurrence of the $C2/c$ type ordering in Cd_6Ca .¹¹ Furthermore, concerning the number of possible orientations in the disordered state, two orientations of the Cd_4 tetrahedron randomly occur in the case of the $C2/c$ -type ordering, whereas six orientations occur for the $C2/m$ -type ordering, leading to different transition entropies of $k_B \ln 2$ and $k_B \ln 6$ per icosahedral cluster, respectively. Of these two orderings, the transition entropy of $\sim k_B \ln 2$ obtained from the specific heat measurement⁶ also supports an occurrence of the $C2/c$ -type order below 100 K for Cd_6Ca , that is, the Cd_4 tetrahedra are ordered in an antiparallel fashion along $[110]$ direction below 100 K in such a way that twofold axes of the Cd_4 tetrahedra are parallel to the b axis of the monoclinic lattice. Such a transition in a metal is reminiscent of orientational transitions in molecular solids.

This research was supported by Core Research in Environmental Science and Technology (CREST), Japan Science and Technology Corporation.

- ¹R. Tamura, Y. Murao, S. Takeuchi, M. Ichihara, M. Isobe, and Y. Ueda, *Jpn. J. Appl. Phys., Part 2* **41**, L524 (2002).
- ²R. Tamura, K. Edagawa, Y. Murao, S. Takeuchi, K. Suzuki, M. Ichihara, M. Isobe, and Y. Ueda, *J. Non-Cryst. Solids* **334&335**, 173 (2004).
- ³T. B. Massalski, H. Okamoto, P. R. Subramanian, and L. Kacprzak, *Binary Alloys Phase Diagrams*, edited by T. B. Massalski, H. Okamoto, P. R. Subramanian, and L. Kacprzak (The Materials Information Society, Metals Park, Ohio, 1996), Vol. 1, p. 899; Vol. 2, p. 1044.
- ⁴A. P. Tsai, J. Q. Guo, E. Abe, H. Takakura, and T. J. Sato, *Nature (London)* **408**, 537 (2000).
- ⁵J. Q. Guo, E. Abe, and A. P. Tsai, *Phys. Rev. B* **62**, R14605 (2000).
- ⁶R. Tamura, K. Edagawa, C. Aoki, S. Takeuchi, and K. Suzuki, *Phys. Rev. B* **68**, 174105 (2003).
- ⁷A. Palenzona, *J. Less-Common Met.* **25**, 367 (1971).
- ⁸G. Bruzzone, *Gazz. Chim. Ital.* **102**, 234 (1972).
- ⁹C. P. Gomez and S. Lidin, *Phys. Rev. B* **68**, 024203 (2003).
- ¹⁰L. D. Landau and E. M. Lifshitz, *Statistical Physics*, 3rd ed. (Pergamon, Oxford, 1980), Pt. 1, Chap. XIV.
- ¹¹Recently, Saitoh *et al.*, performed convergent beam electron diffraction experiments on Cd₆Ca below 100 K and found that not a mirror but a glide plane (*c* glide) perpendicular to the *b* axis exists for the low-temperature phase. Their result is of great importance to the present scenario since the existence of the *c* glide lends support to the C2/*c*-type ordering of the central Cd₄ tetrahedra among the two cases.